

Supporting Information

Improved hydrothermal stability of Pd particles on nitrogen-doped
carbon supports

*Jiajie Huo,^{ab} Pu Duan,^{bc} Hien N. Pham,^{bd} Yee Jher Chan,^a Abhaya K. Datye,^{bd} Klaus Schmidt-
Rohr,^{bc} Brent H. Shanks^{ab*}*

^aDepartment of Chemical and Biological Engineering, Iowa State University, Ames, Iowa 50011,
United States

^bCenter for Biorenewable Chemicals, Iowa State University, Ames, Iowa 50011, United States

^cDepartment of Chemistry, Brandeis University, Waltham, Massachusetts 02453, United States

^dDepartment of Chemical and Biological Engineering and Center for Microengineered Materials,
University of New Mexico, Albuquerque, New Mexico 87131, United States

* E-mail: bshanks@iastate.edu Phone: +1 (515) 294-1895.

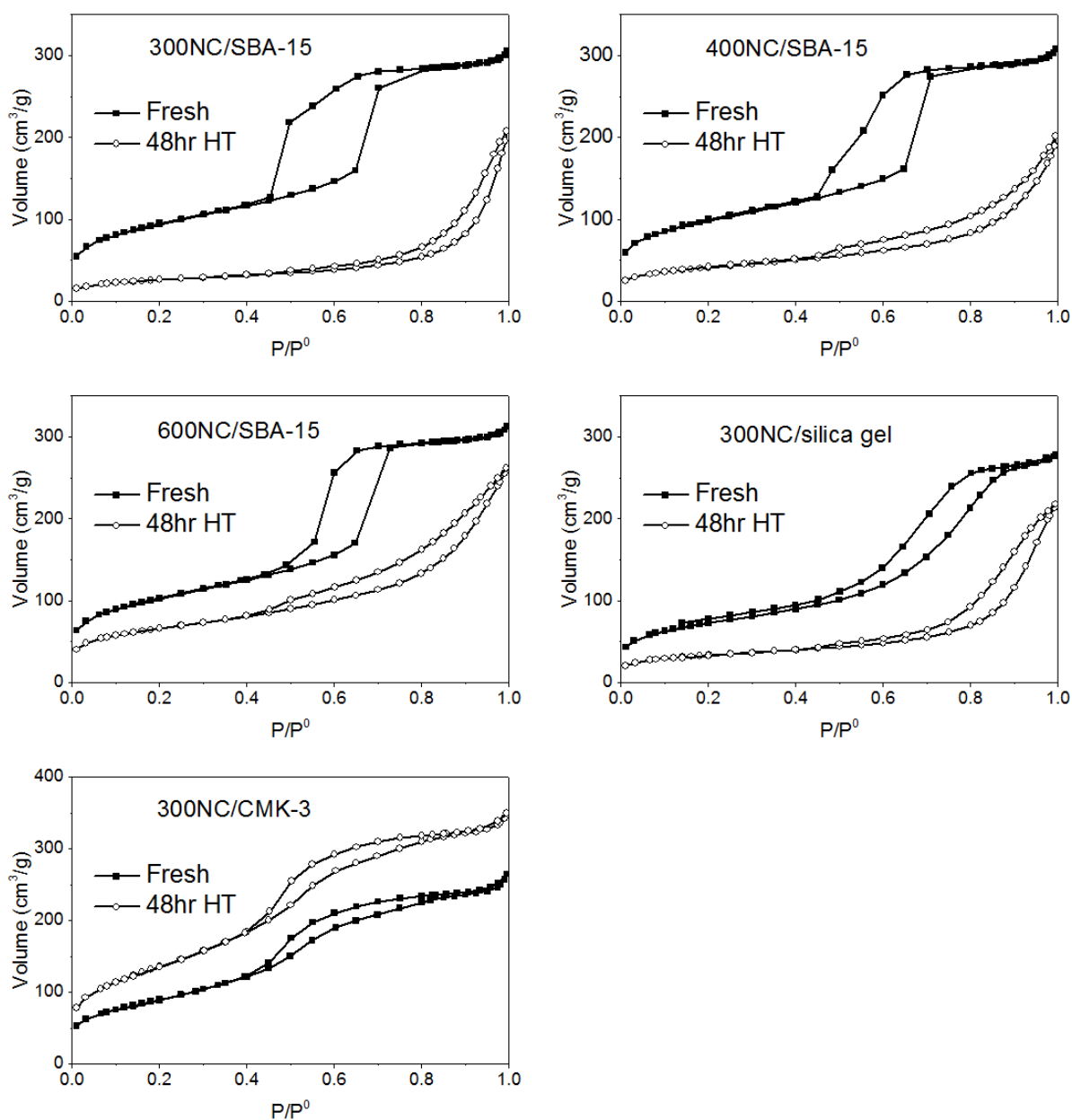


Fig. S1. Nitrogen physisorption isotherms of 300NC/SBA-15, 400NC/SBA-15, 600NC/SBA-15, and 300NC/silica gel before and after 48 h of hydrothermal treatment. (HT: hydrothermal treatment)

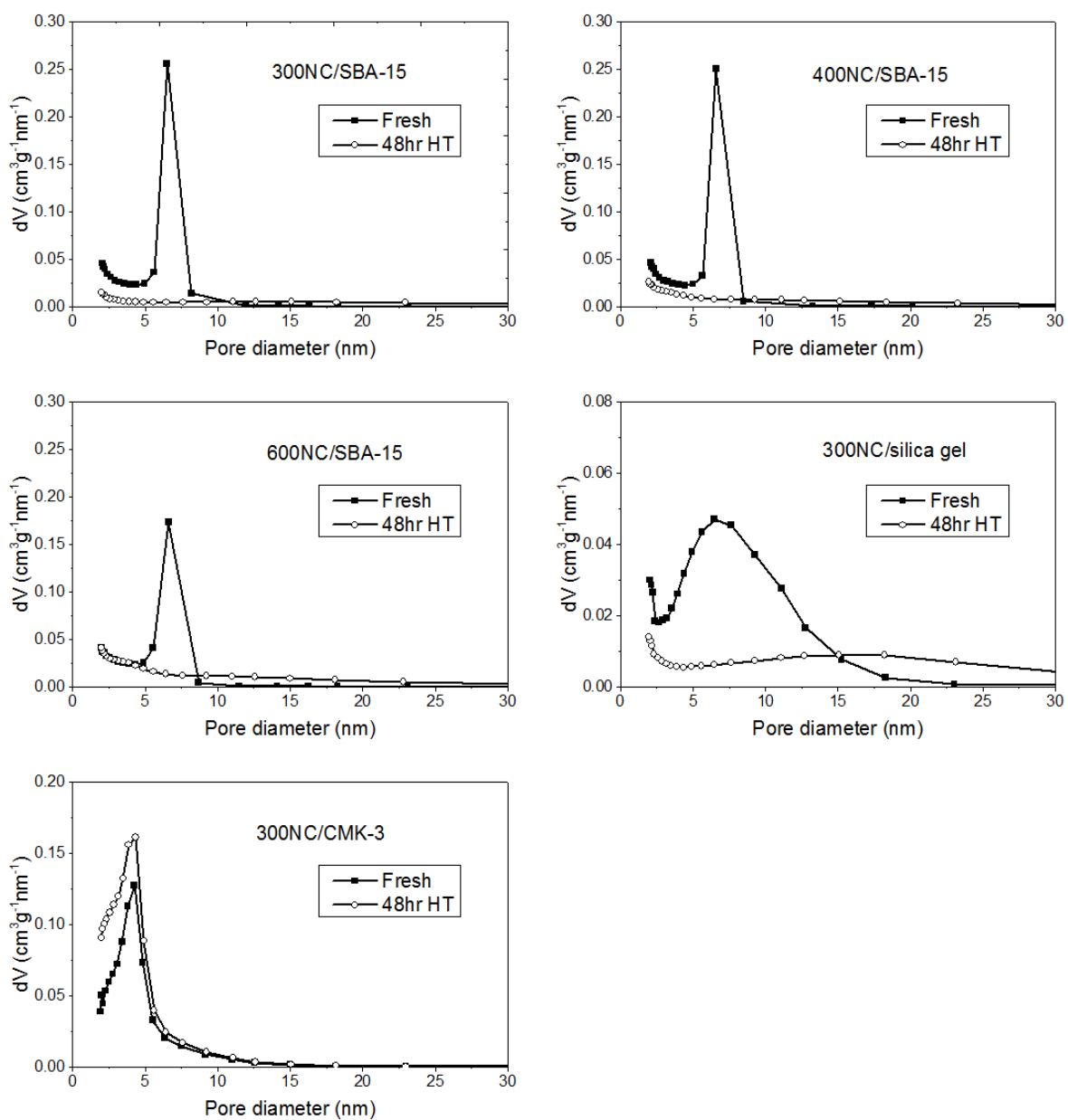


Fig. S2. Pore size distribution curves of 300NC/SBA-15, 400NC/SBA-15, 600NC/SBA-15, 300NC/silica gel, and 300NC/CMK-3 before and after 48 h of hydrothermal treatment. (HT: hydrothermal treatment)

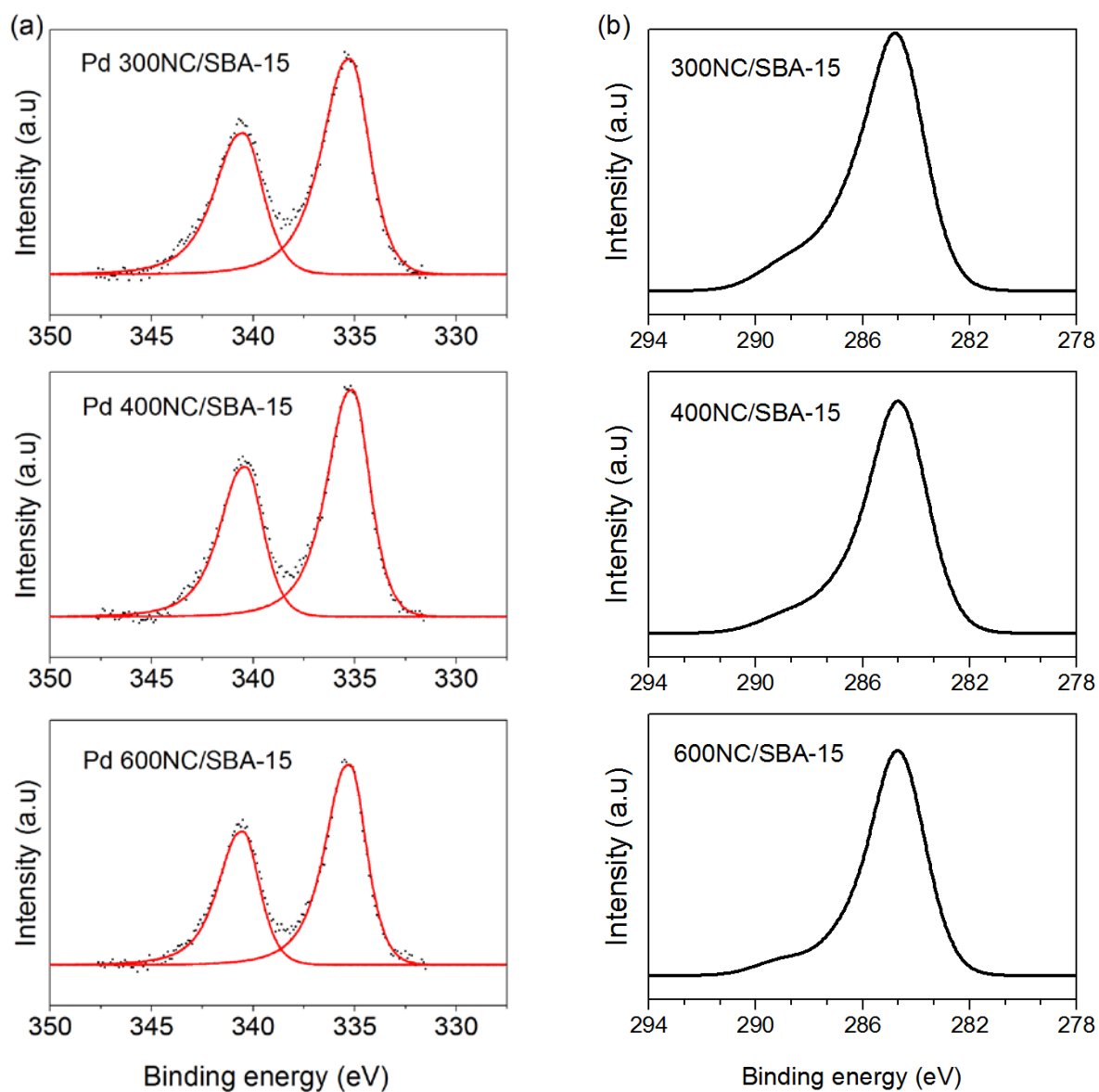


Fig. S3. Pd 3d XPS (a) and C 1s (b) spectra of Pd 300NC/SBA-15, Pd 400NC/SBA-15, and Pd 600NC/SBA-15.

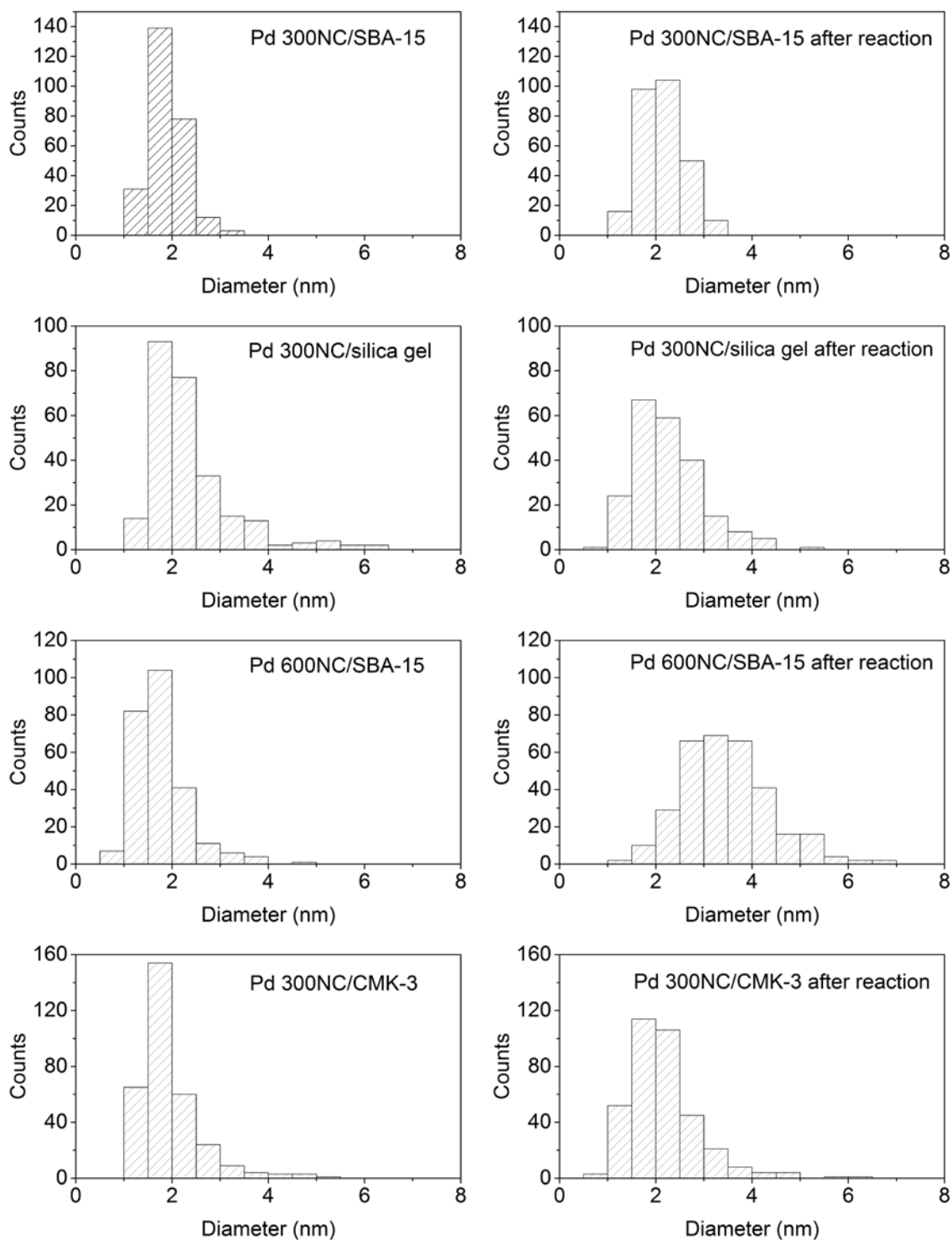
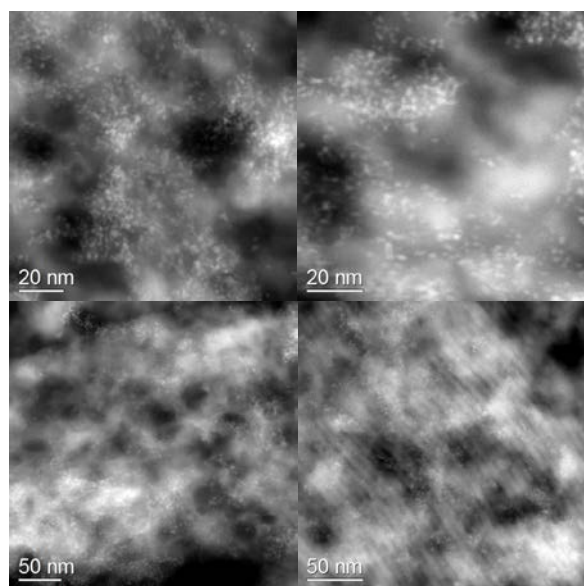


Fig. S4. Particle size distribution of Pd 300NC/SBA-15, Pd 300NC/silica gel, Pd 600NC/SBA-15, and Pd 300NC/CMK-3 before and after 48 h of flow reaction.

Pd 300NC/SBA-15 after 10 h reaction



Pd 600NC/SBA-15 after 10 h reaction

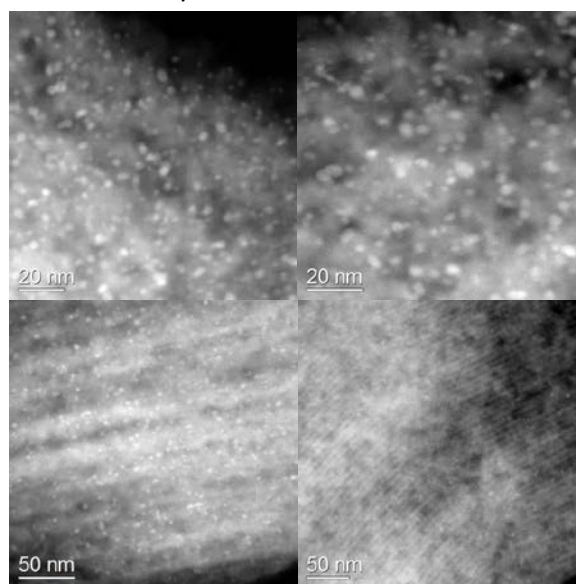
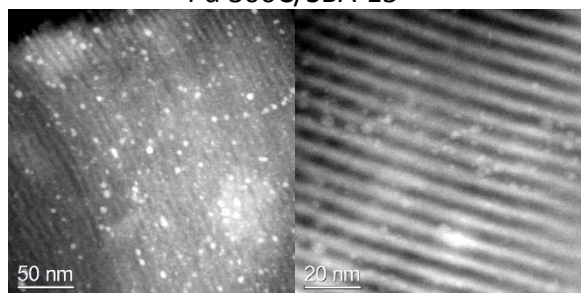
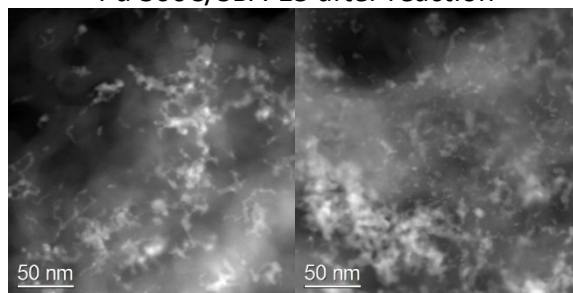


Fig. S5. HAADF-STEM images of Pd 300NC/SBA-15 and Pd 600NC/SBA-15 after 10 h of flow reaction at 130°C and 750 psi H₂.

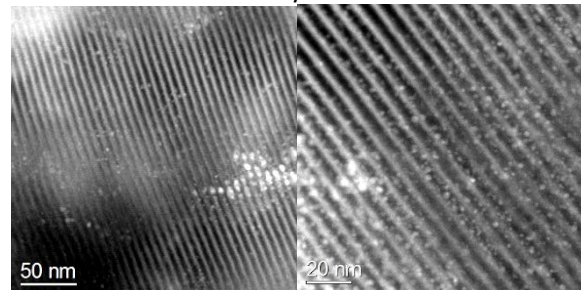
Pd 300C/SBA-15



Pd 300C/SBA-15 after reaction



Pd 600C/SBA-15



Pd 600C/SBA-15 after reaction

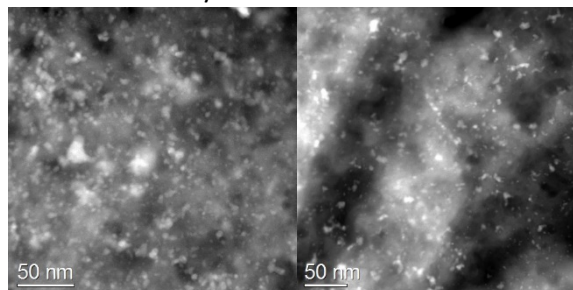


Fig. S6. HAADF-STEM images of Pd 300C/SBA-15 and Pd 600C/SBA-15 before and after 48 h of flow reaction.

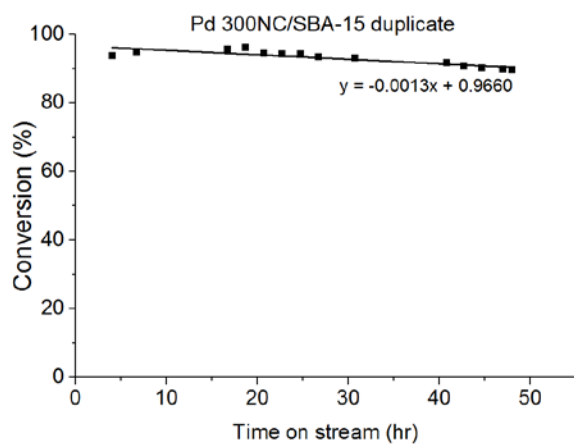


Fig. S7. Duplicate of continuous flow hydrogenation of furfural on Pd 300NC/SBA-15 at 130°C and 750 psi H₂ for 48 h.

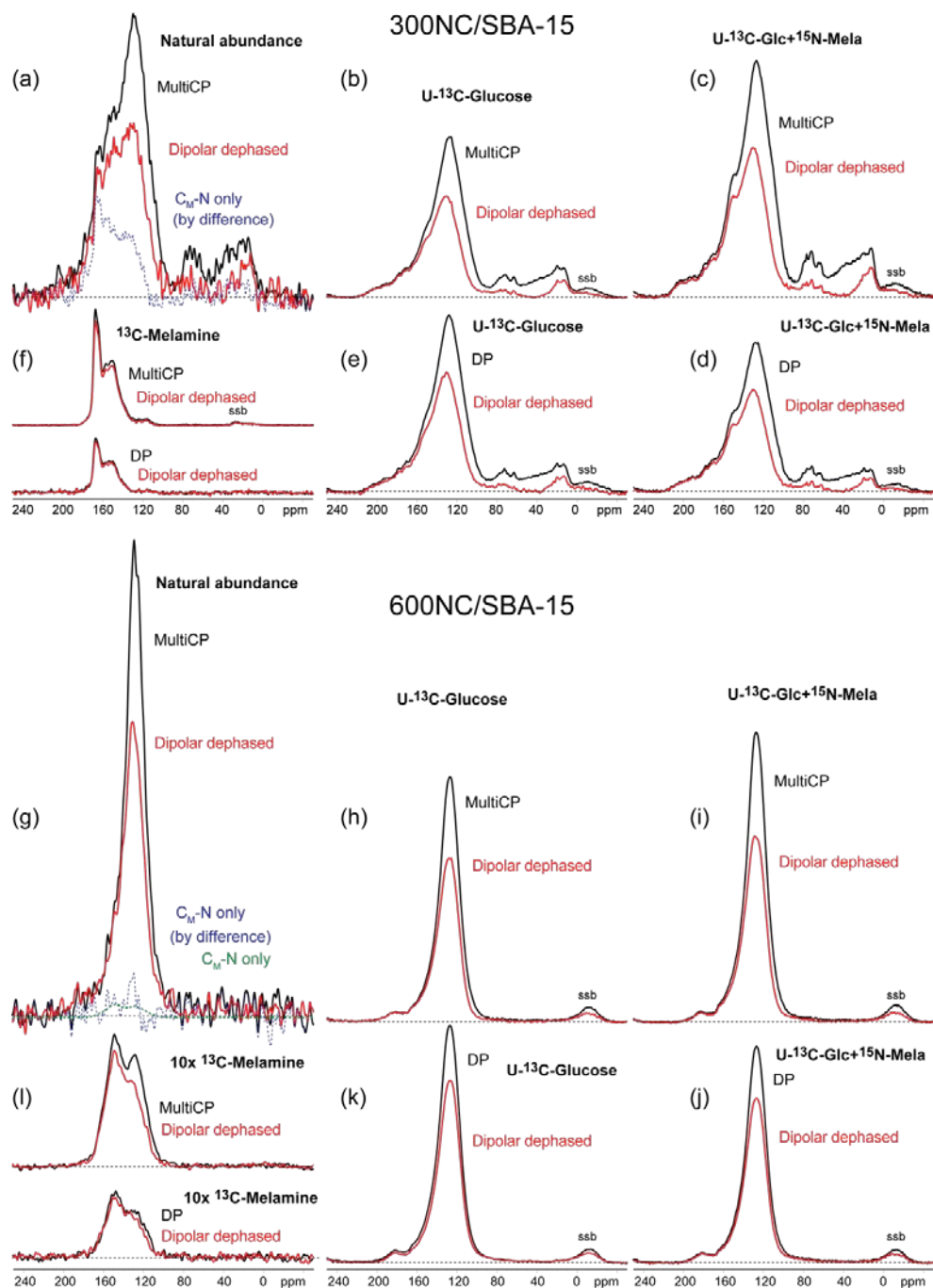


Fig. S8: Overview of quantitative ^{13}C NMR spectra of several NC/SBA-15 materials made with different isotopic enrichments. Spectra are scaled to correct for sample mass, the ^{13}C enrichment level, and the number of scans. (a-e) Spectra of three nominally equivalent 300NC/SBA-15 samples: (a) Unlabeled (^{13}C in natural abundance of 1.1%), (b) from ^{13}C -enriched glucose. Top row: multiCP, bottom row: DP spectra. (f) Spectra of carbon in 300NC/SBA-15 derived from melamine. (g-k) Spectra of three nominally equivalent 600NC/SBA-15 samples. Top row: multiCP, bottom row: DP spectra. (l) Spectra of carbon in 600NC/SBA-15 derived from melamine.

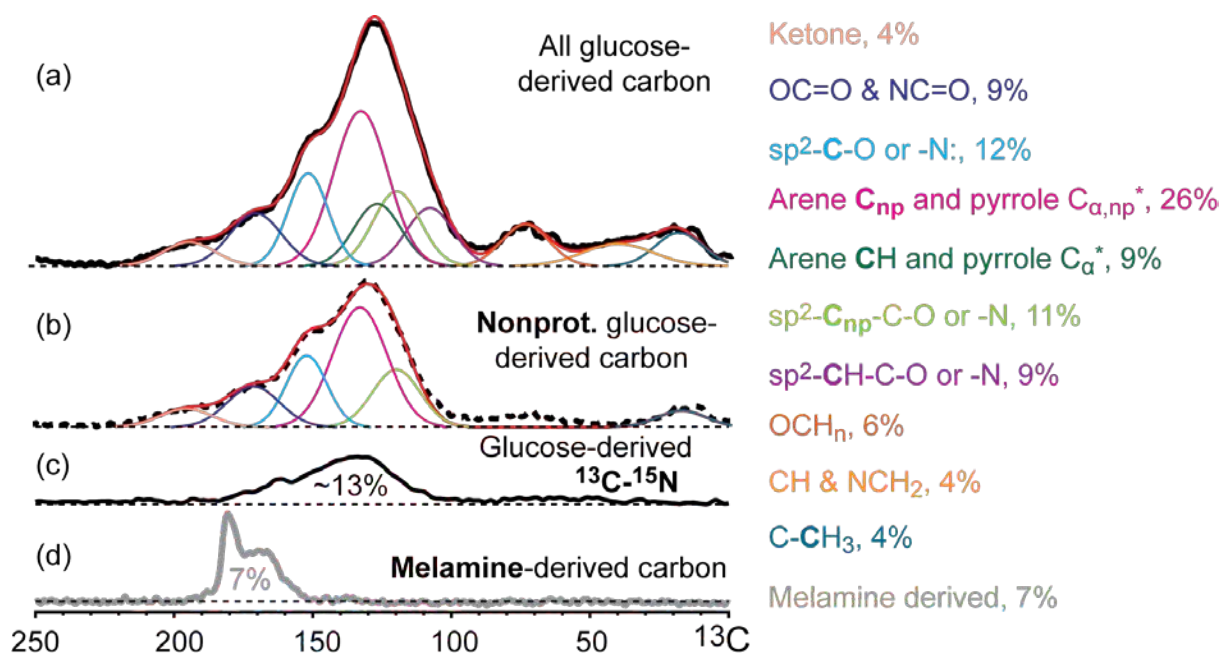


Fig. S9. Deconvolution of the (a) DP and (b) DP/dipolar dephasing ^{13}C NMR spectra of NC300/SBA-15 made from ^{13}C -enriched glucose. (c) Corresponding $^{13}\text{C}^1$ REDOR difference spectrum of the same material, showing signals of glucose-derived carbon bonded to ^{15}N . The deconvolution of this spectrum is shown in Fig. 6. (d) Corresponding spectrum of carbon derived from ^{13}C -enriched melamine.

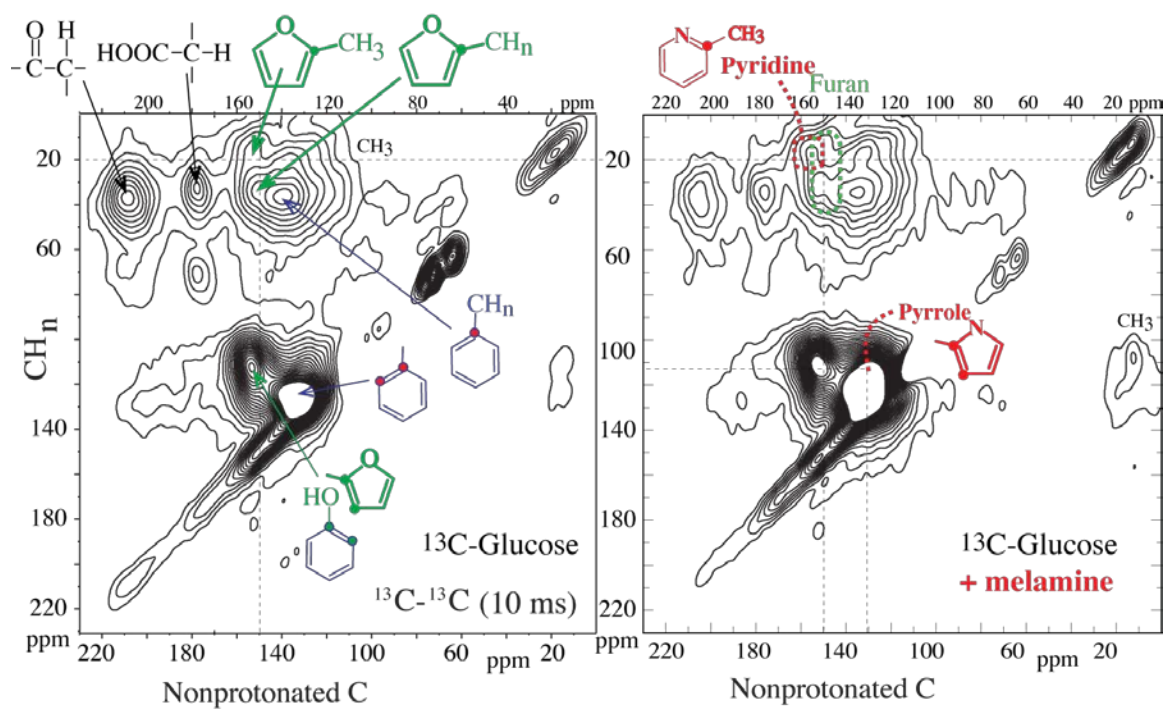


Fig. S10. Spectrally edited ^{13}C - ^{13}C correlation spectra of (left) a reference material 300C/SBA-15 made from ^{13}C -glucose without melamine and (right) 300NC/SBA-15 made from ^{13}C -glucose and melamine. Signals of protonated C along the vertical axis are correlated with peaks of nonprotonated C and mobile segments along the horizontal axis. Additional distinctive signals of C near N in the material with melamine are labeled.

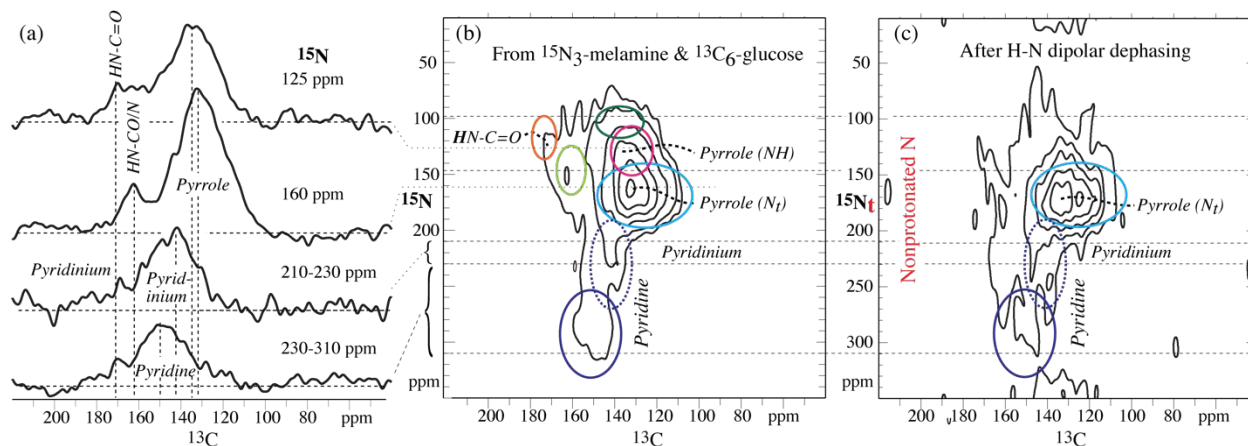


Fig. S11. ^{15}N - ^{13}C correlation spectra of 300NC/SBA-15 made from ^{13}C -glucose and $(^{15}\text{NH}_2)_3$ -labeled melamine, facilitating assignment of the ^{15}N NMR signals. (a) Cross sections along the ^{13}C dimension, at 125 and 160 ppm in the ^{15}N dimension and partial projections from 210-230 ppm and 230-310 ppm, as indicated (top to bottom), from the 2D spectrum in b). (b) Contour plot of the full 2D spectrum. (c) Corresponding spectrum of nonprotonated N_t , after suppression of NH by recoupling of the ^{15}N - ^1H dipolar interaction. The color coding of the ellipses is the same as in Fig. 6.

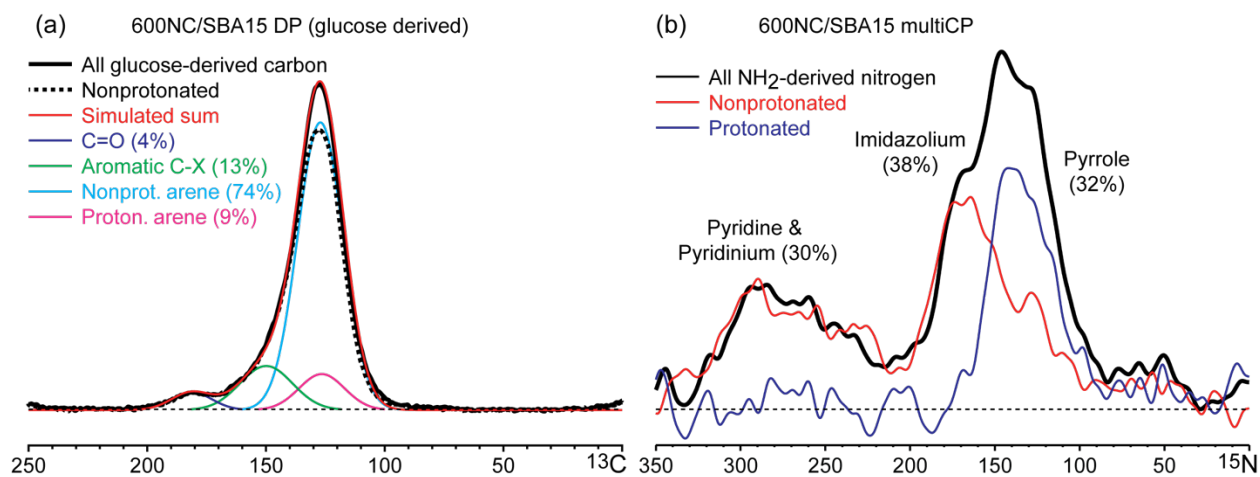


Fig. S12. Analysis of NMR spectra of 600 NC/SBA-15. (a) Deconvolution of the quantitative DP ^{13}C NMR spectrum. (b) Assignments of multiCP and multiCP/dipolar dephasing ^{15}N spectra and fractional peak areas of the main components.

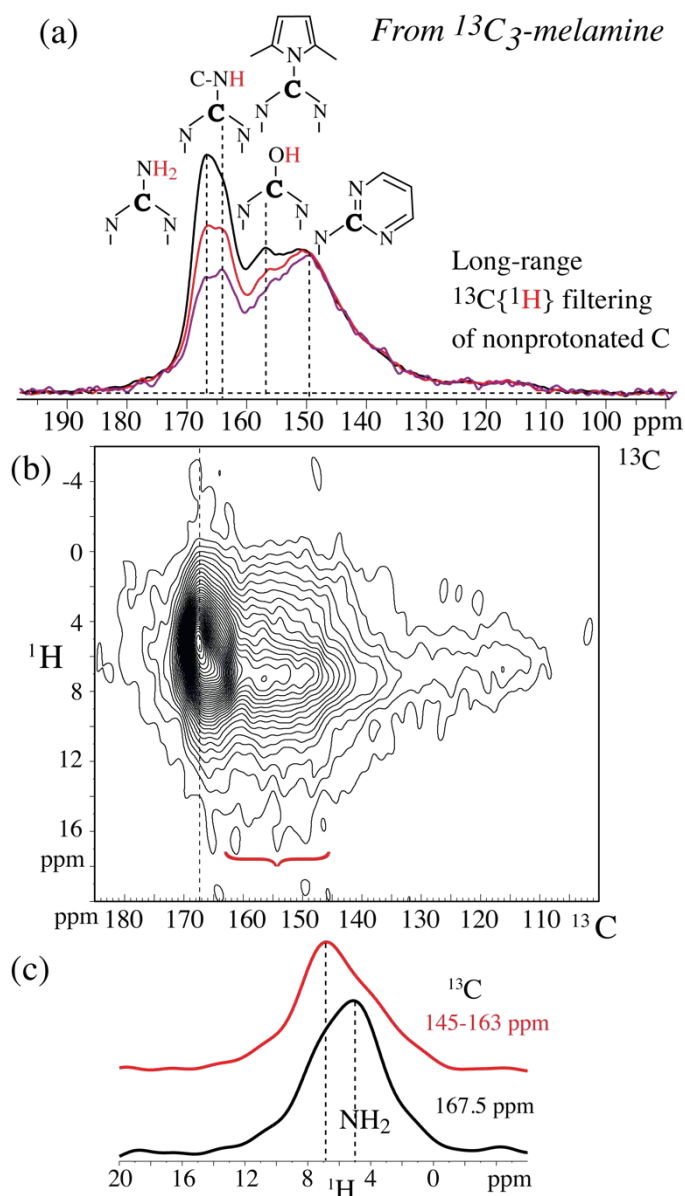


Fig. S13. Spectra of 300NC/SBA-15 made from unlabeled glucose and $^{13}\text{C}_3$ -melamine. (a) Series of ^{13}C NMR spectra after long-range ^{13}C dipolar dephasing, reflecting relative proximity of carbons to the nearest protons: full (top trace), after 0.38 ms (middle trace, red line), and after 0.57 ms (bottom trace, purple line) of long-range ^{13}C dipolar dephasing. The spectra after dephasing have been scaled vertically by 1.9 and 4.4, respectively, to match in intensity at 150 ppm. The assignment of the signal at 164 ppm to carbon bonded to NH is confirmed by ^1H - ^{13}C NMR, see Fig. S5. (b) ^1H - ^{13}C heteronuclear correlation spectrum and (c) cross sections/partial projections. The distinct difference in the ^1H chemical shift associated with ^{13}C resonating at 164 vs. 167.5 ppm is attributed to NH vs. NH_2 .

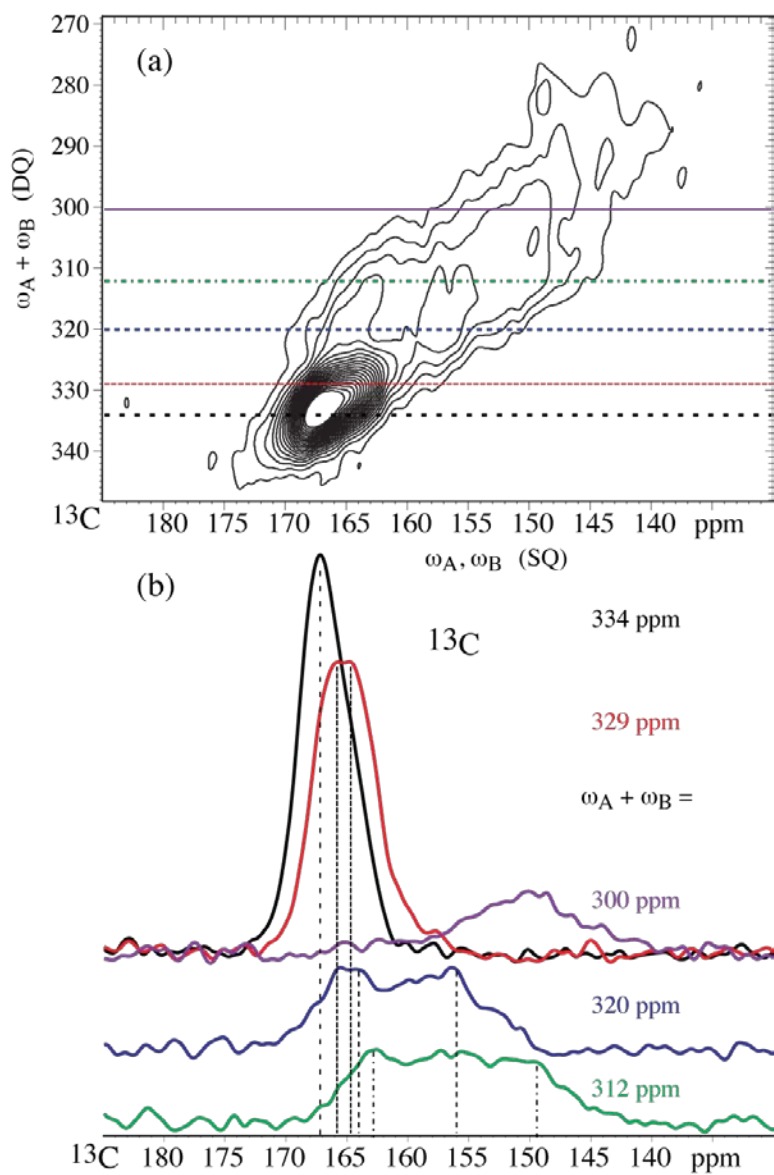


Fig. S14. DQ/SQ ^{13}C - ^{13}C correlation of 300NC/SBA-15 made from unlabeled glucose and $^{13}\text{C}_3$ -melamine. (a) 2D spectrum; (b) Cross sections at the double-quantum frequencies indicated in a), with correlated frequencies indicated by vertical lines.

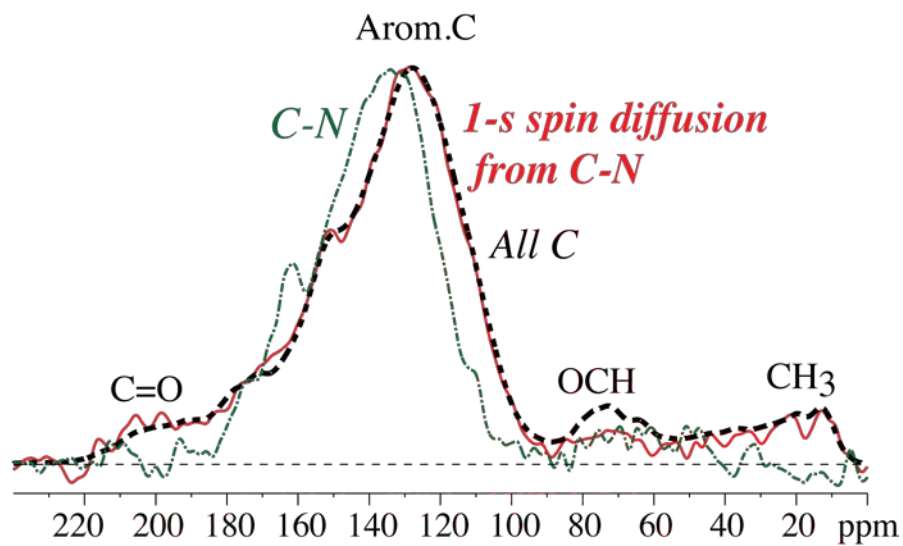


Fig. S15. Spectra of ^{13}C near ^{15}N in 300 NC/SBA-15, on the 0.2-nm and 3-nm scales. Dash-dotted green line: ^{13}C bonded to ^{15}N . Solid red line: same after 1 s of ^{13}C spin diffusion, showing signal of ^{13}C within ~ 3 nm from ^{15}N . The signal of all C measured under the same conditions is shown for reference (dashed line), scaled to match the largest peak.

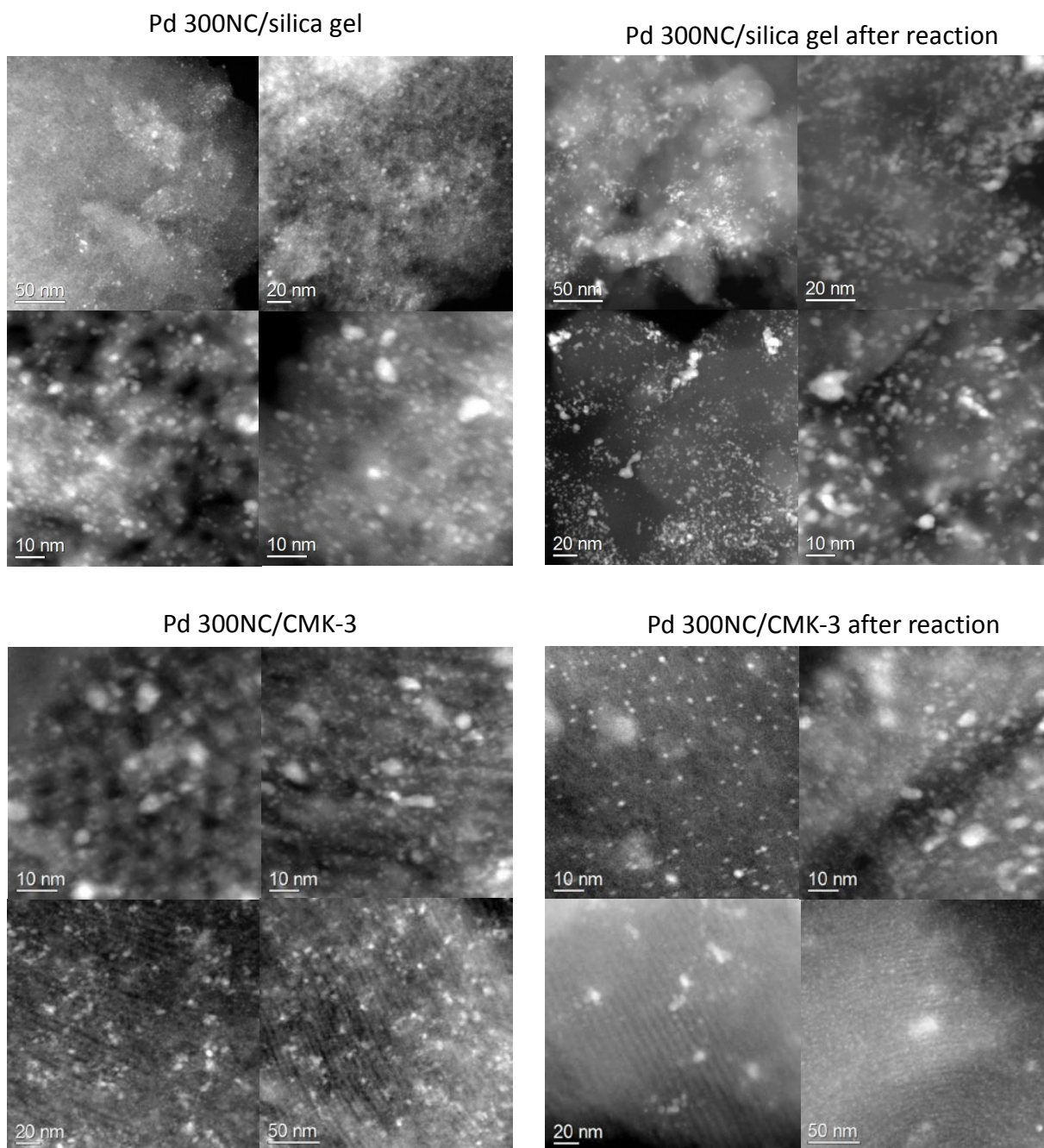


Fig. S16. HAADF-STEM images of Pd 300NC/silica gel, and Pd 300NC/CMK-3 before and after 48 h of continuous flow reaction.

¹⁵N functional group analysis of fresh 300NC/SBA-15 by NMR

In 300NC/SBA-15, the major form of nitrogen (ca. 27%) is substituted N of pyrrole or imidazolium resonating near 170 ppm, with nitrogen not bonded to hydrogen, according to the spectral editing in Fig. 5b and S11c. The corresponding major ¹³C resonance near 130 ppm, representing the maximum in the 2D spectra in Fig. 6 and S11, confirms the assignment. Pyrrole without substitution of N has a similar aromatic ¹³C chemical shift but the nitrogen resonates near 125 ppm and is bonded to ¹H (see Fig. S11b,c). The structure suggests that the nitrogen has detached from the triazine ring of melamine.

The next most abundant form of nitrogen is pyridinium, visible as a broad shoulder around 220 ppm in Fig. 5b and 6, and merging with the pyridine/pyrimidine band, which extends out to 320 ppm. The pyridinium nitrogen presumably remains bonded to melamine carbon after glucose has “wrapped around” the melamine amine. Pyrimidine could form by incorporation of triazine nitrogen and carbon of melamine and an NH₂ nitrogen into a pyrimidine ring (see Fig. S13a). By contrast, pyridinic N would have to be incorporated individually into glucose-derived aromatic rings, originating from NH₂ detached from the melamine (strictly speaking, triazine) ring and being replaced by OH (¹³C resonance near 157 ppm in Fig. S13).

Amide and NCX₂ groups, with around 10% abundance each and with N mostly bonded to hydrogen, are best identified by the partially resolved peaks of their carbon atoms in Fig. 6. While amide, NC=O, linking various aromatic or aliphatic units is a major component of lower-temperature Maillard reaction products, it is apparently less abundant in the synthesis at 300°C. NCX₂ groups with a distinctive ¹³C resonance near 160 ppm contain sp²-hybridized carbon bonded to nitrogen and two other heteroatoms, of which one is double-bonded. Ureido (N₂C=O)

and, less likely, guanidino ($\text{N}_2\text{C}=\text{N}$) groups are typical examples.¹ The melamine $\text{N}_2\text{C}=\text{N}$ resonances also fall into this category, but formation of a melamine ring from glucose carbon seems relatively unlikely. The ~ 160 ppm ^{13}C and 130-160 ppm ^{15}N chemical shifts also match those of cyclic amides with a bond to another sp^2 -hybridized carbon, for instance in uracil.¹

References

1. X. W. Fang, J. D. Mao, R. M. Cory, D. M. McKnight and K. Schmidt-Rohr, *Magn. Reson. Chem.*, 2011, **49**, 775-780.